

# Ions Traces Substitution in Stoichiometric Calcium-Hydroxyapatite: Structural Analysis by Rietveld Refinement

M. Ellassfour, B. El ouatli\*, F. Abida, M. Jamil, A. Kheribech, Z. Hatim  
Team of Electrochemistry and Biomaterials, Department of Chemistry, Faculty of Sciences,  
University of Chouaib Doukkali, El Jadida, Morocco

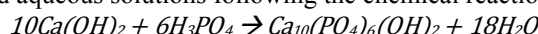
## Abstract

Impact of trace ions as  $Mg^{2+}$ ,  $Na^+$ ,  $Sr^{2+}$ ,  $SO_4^{2-}$ , and  $CO_3^{2-}$  on stoichiometric hydroxyapatite ( $Ca_{10}(PO_4)_6(OH)_2$ ) crystal structure is investigated. The first four ions are brought by the raw material while the carbonate group is due to contamination by air. The powders were prepared, under industrial conditions, at  $22^\circ C$  from aqueous solutions by reaction between the calcium hydroxide and orthophosphoric acid at pH from 7 to 7.5. Two samples of hydroxyapatite powder, which differ by the content of ions trace, calcined at  $1100^\circ C$  have been investigated by X-ray powder patterns fitting methods. Results showed that in the absence of ion traces, the partial replacement of  $PO_4^{3-}$  by  $CO_3^{2-}$  groups leads to the - relaxation of the lattice by creation of vacant calcium (Ca1 and Ca2) sites, - reduction of the cell parameters, and new lattice rearrangement with lower  $PO_4$  distortion index, ( $D_{ind} = 0.488$ ) compared to the calculated theoretical value ( $D_{ind}=3.079$ ). For trace ions incorporated hydroxyapatite sample, the presence of traces cation favors the incorporation of carbonate ions. Coupled substitution on Ca2 and P position affect neither theoretical structure nor thermal stability of the hydroxyapatite but causes vacancies creation in calcium (Ca1) and oxygen (O1 and O3) sites. This structural change leads to a slight lattice distortion ( $D_{ind}=3.204$ ). Composition and microstructure of analyzed materials appear very promising for biological applications.

**Keywords:** Biomaterials, Calcium-hydroxyapatite, Traces ions, Crystalline structure.

## 1. Introduction

In recent years, significant research effort has been devoted to developing powder of hydroxyapatite ( $Ca_{10}(PO_4)_6(OH)_2$ , HAP) because of their potential application in many interdisciplinary fields including chemistry, biology and medicine [1-3]. The prepared hydroxyapatite, due to the same structure of the natural bone, has good compatibility with the human organism, and is widely used in medical applications as implant or as coating on prosthesis [4-6]. Hydroxyapatite is used in the form of powder, granule, block or the injectable paste, its uses requiring heat treatment at high temperature [7, 8]. Several techniques have been used for HAP powders preparation (wet synthesis, solid-state reaction and hydrothermal methods etc) [9-11] and materials with various composition, stoichiometry, and crystallinity, have been obtained. These properties affect the physical and chemical properties, such as phase thermal stability bioactivity and dissolution behaviour [12, 13]. In our laboratory we are interested in the preparation of calcium-hydroxyapatite powder under industrial conditions and with a controlled chemical composition and crystallographic structure. The powders are prepared at room temperature from supersaturated aqueous solutions following the chemical reaction:



The used of this simple and non polluting method, appears to be very promising for the preparation of hydroxyapatite powders in industrial scale. The purity, stoichiometry and the physicochemical properties of produced powder are influenced by operating parameters as flow rate of reagent, stirring rate, pH and temperature. But the purity of the raw materials, especially  $Ca(OH)_2$  which still contains traces of ions, have a great influence on the purity, thermal stability and the physicochemical properties of the final product [14,15]. The limit of trace ions is not known and few works were interested in the influence study of trace ions on the physicochemical properties of calcium hydroxyapatite. The aim of the present work is the studying the effect of trace elements as  $Mg^{2+}$ ,  $Na^+$ ,  $Sr^{2+}$ ,  $SO_4^{2-}$ , and  $CO_3^{2-}$  on the structural atomic rearrangement in prepared hydroxyapatite. The first four ions are brought by the raw material whereas the carbonate presence is due to contamination by air. It is important to note that these elements are often detected, with different concentrations, during chemical controls of synthesized hydroxyapatite. Two samples, which differ by the content of ion trace, calcined at  $1100^\circ C$  have been investigated by X-ray powder pattern fitting methods with the means of FULLPROF WINPLOTR 2011 program. Crystallographic data available in database will be designated as theoretical values.

## 2. Preparation method

500g of pure reference sample and trace ions incorporated hydroxyapatite powders were synthesized by reaction between the calcium hydroxide and orthophosphoric acid under industrial conditions as reported by Abida F. [14]. In the present experiment, the reaction system was open to air. The appropriate amount of orthophosphoric acid solution was added into  $Ca(OH)_2$  suspension using an automatic titration with vigorous stirring. The molar ratio

calcium/phosphorus of the reagents is fixed at 1.667 (molar ratio of the stoichiometric hydroxyapatite). The reaction mixture is carried out at 22 °C and the pH from precipitation is from 7 to 7.5. The resulting precipitate was aged for 12 h then filtered, dried and calcined at 1100°C for 3h.

In order to obtain trace ions incorporated hydroxyapatite powder, the sample is prepared from pure raw material with pharmaceutical grade. This sample will be designated as HAP. A pure reference sample of hydroxyapatite powder is prepared under the same conditions but from the pure raw material with analytical grade. This reference will be designated as HAPr.

### 3. Characterization techniques

#### 3.1 Chemical characterization

Chemical analyses are carried out on the calcined powder at 1100°C. The formed phases were identified by means of the atomic ratios Ca/P using the infrared spectroscopy (PerkinElmer FTIR 1600), and the X-ray diffraction (Siemens 5000). Chemical tests were performed to detect traces of lime (CaO). The chemical analysis of final materials was determined by atomic emission spectrophotometer, argon plasma and the inductive coupling (ICP-AES) (Thermo Jarrel Ash. Atom Scan 16). Carbonate content is determined by HCN analysis.

#### 3.2 Thermal analysis

Thermal Analysis was performed on Netzsch STA 429 facility with a conventional Pt/Rh sample holder capable of simultaneous recording of thermogravimetric (TG), derivative thermogravimetric (DTG) in the temperature range of 20 to 1450°C. The measurements of the powder sample (30 mg) were recorded under ambient pressure and at a heating rate of 10°C/min.

#### 3.3 Microstructural refinement

The X-ray powder data were collected on D5000 operating in step scan mode using Cu radiation. X-ray data were collected between 10° and 90° with a 0.02° 2θ step and counting 15s by step. FullProf code [16], were used to perform Rietveld refinements. Refined values (a and c cell parameters, atomic positions, site occupancies, thermal parameters) of stoichiometric hydroxyapatite [17] were used as the starting model. The pseudo-Voigt function was used to present the individual reflection profiles. In final step of the refinement, all atomic positions and site occupancies were refined simultaneously with atom displacement factor. In the last cycle of refinement, 33 parameters structural and non-structural were optimized.

The distortion of the lattice can be calculated from the tetrahedron PO<sub>4</sub> according to the Eqs (1).  $D_{ind}$  represents the deviation of the tetrahedron PO<sub>4</sub> in the structure and terms  $\theta$  represents OPO angle.

$$D_{ind} = \frac{\sum_{i=1}^{i=6} (\theta_i - 109.17)^2}{6} \quad (1)$$

From the refinement, the  $R_c$  hydroxyl channel radius is calculated using Eqs (2).

$$R_c = \frac{d(Ca_2 - Ca_2)}{2} \operatorname{tg} \frac{\pi}{6} \quad (2)$$

$d(Ca_2-Ca_2)$  stands for a bond length.

## 4. Results

### 4.1 Chemical composition

Chemical analysis was carried out on reference sample (HAPr) and sample with ions trace (HAP) and the results are compared to available data designated, in this work, as theoretical values (HAP<sub>Theo</sub>). For both samples, the calculated Ca/P molar ratio is close to the theoretical values of the stoichiometric hydroxyapatite as reported in Table1. The considered trace ions (Mg<sup>2+</sup>, Na<sup>+</sup>, Sr<sup>2+</sup> and S<sup>2-</sup>) concentrations are listed in this table and total mass fraction of the trace elements was 612 ppm for the HAP sample. Other trace ions as Fe<sup>2+</sup>, Zn<sup>2+</sup>, Al<sup>3+</sup>... were detected, but with concentrations of less than 10 ppm. The same trace elements were detected in the reference sample (HAPr) with total mass fraction from 169 ppm. Mg<sup>2+</sup> and Sr<sup>2+</sup> ions are brought by the calcium dihydroxide while the Na<sup>+</sup> and S<sup>2-</sup> are brought by orthophosphoric acid and calcium dihydroxide. The details of chemical analysis of raw materials are reported by Abida F. [14].

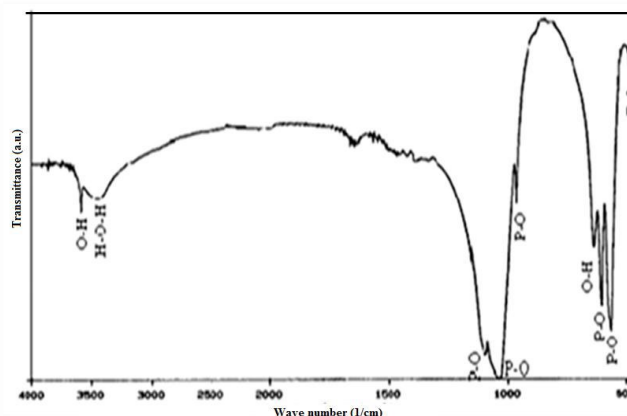
Reference sample (HAPr) and sample with ions trace (HAP) are precipitated in industrial conditions at room temperature at pH from 7 to 7.5 and under air atmosphere which leads to product contamination by air carbonate. For prepared powders the carbonate ions (CO<sub>3</sub><sup>2-</sup>) are detected with concentration from 0.33 (HAPr) and 0.46 wt. % (HAP).

**Table 1:** Chemical composition of HAPr, trace ions substituted and theoretical Hydroxyapatite

Sample	Ca (%)	P (%)	Ca/P (Molar ratio)	CO <sub>3</sub> <sup>2-</sup> (%)	Mg <sup>2+</sup> (ppm)	Na <sup>+</sup> (ppm)	Sr <sup>2+</sup> (ppm)	S <sup>2-</sup> (ppm)
HAP	38.87 ± 0.54	18.05 ± 0.22	1.664 ± 0.005	0.46	111	179	119	203
HAP <sub>r</sub>	39.92 ± 0.54	18.40 ± 0.22	1.677 ± 0.005	0.33	70	64	35	-
HAP <sub>THE</sub>	39.90	18.50	1.666	-	-	-	-	-

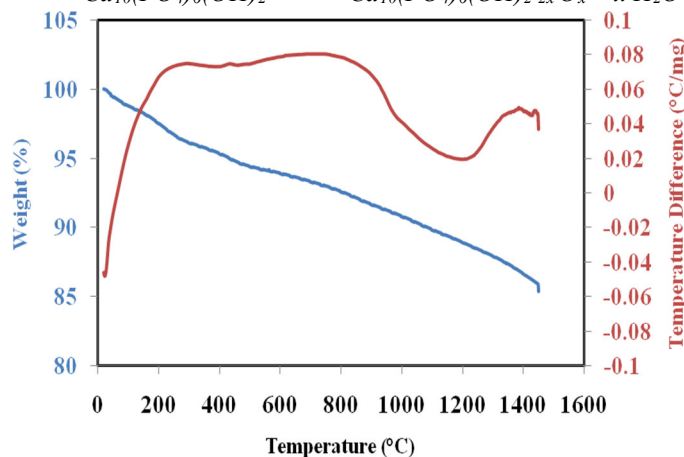
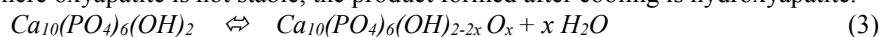
#### 4.2 Infrared spectroscopy and gravimetric analysis

The infra-red spectre of calcined powder with ions traces (HAP), reported in Figure 1, shows on one hand the presence of only one well-crystallized phase of the hydroxyapatite, and, other hand the absence of carbonate and other calcium phosphates such as tricalcium phosphates or calcium oxide. The similar results are obtained with reference sample (HAPr).



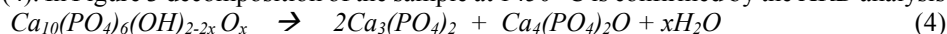
**Figure 1:** FTIR spectra of trace ions substituted hydroxyapatite powder calcined at 1100°C

TGA DTA measurements on HAP sample reported in Figure 2 showed, firstly, weight loss between 950°C to 1300°C associated with a large endothermic effect, which is characteristic of the HAP dehydroxylation accompanied by formation of oxyapatite according to the reaction (3). The thermal treatment of the products is carried out in air atmosphere where oxyapatite is not stable, the product formed after cooling is hydroxyapatite.



**Figure 2:** ATD/ATG curves of trace ions substituted hydroxyapatite powder (HAP)

At 1450°C, the weight loss accelerated strongly and an endothermic peak was observed indicating the HAP decomposition into both tricalcium phosphate (Ca<sub>3</sub>(PO<sub>4</sub>)<sub>2</sub>) and tetracalcium phosphate (Ca<sub>4</sub>(PO<sub>4</sub>)<sub>2</sub>O) according to the reaction (4). In Figure 3 decomposition of the sample at 1450 °C is confirmed by the XRD analysis.



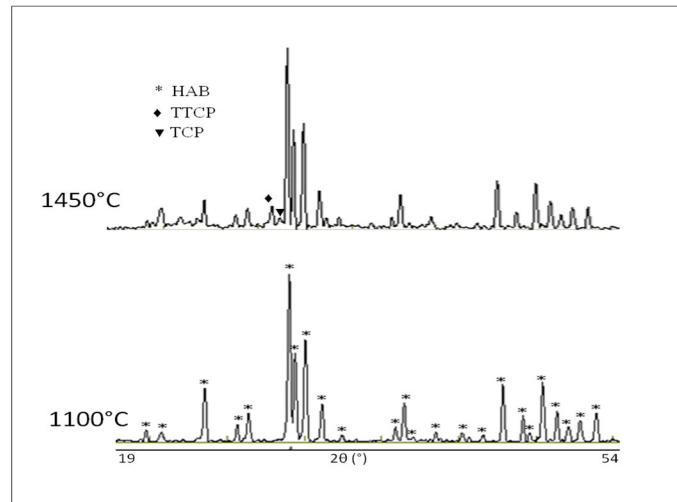


**Figure 3:** X-ray diffraction patterns of trace ions substituted hydroxyapatite powder (HAP) at 1100°C and 1450°C

#### 4.3 X-ray diffraction Patterns and Rietveld refinement

Patterns from X-ray diffraction for both samples HAPr and HAP are displayed in Figure 4 and Figure 5, respectively. They confirm the purity of synthetic hydroxyapatite phase calcined at 1100°C, since they are similar and no significant difference is observed. As conclusion, no influence of trace ions is evidenced. Rietveld refinement is expected to give more information details about trace ions incorporation in the calcium phosphate structure. According to the Rietveld method with the means of FULLPROF WINPLOTR 2011 program [16], the structure refinement was performed. Structure of both HAPr and HAP sample, are refined considering, as starting point, the model of theoretical hydroxyapatite (HAP<sub>THE</sub>) for which we used parameters reported by Sandarsanan and Young [17]. Cell parameters are determined and compared to theoretical values (Table 2). Parameters as  $D_{ind}$  distortion index,  $R_c$  values and volume are gathered in Table 3 and compared to the theoretical values as well. In addition, atom coordinates for both HAPr and HAP sample were refined and listed in Table 5 and 6, respectively. As conclusion concerns structure refinement, both compounds crystallize in hexagonal system with unit cell parameters reported in Table 2.

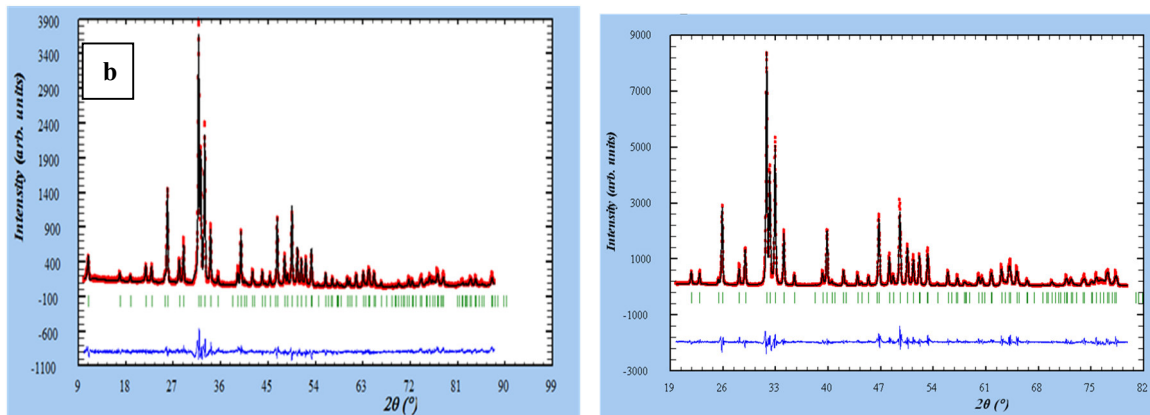


**Figure 4:** X-ray diffraction pattern of (a): hydroxyapatite powder HAPr and (b): trace ions substituted hydroxyapatite powder (HAP) (— experimental; \*\*\* calculated for hexagonal HAP)

**Table 2:** Calculated cell parameters of HAPr, traces ions substituted and theoretical Hydroxyapatite

sample	HAP	HAPr	HAP <sub>THE</sub>
a (Å)=b (Å)	9.408	9.408	9.419
c (Å)	6.872	6.875	6.88
$\alpha(^{\circ})=\beta(^{\circ})$	90.000	90.000	90.000
$\gamma(^{\circ})$	120.000	120.000	120.000
Spatial Group	P 63/m	P 63/m	P 63/m

Cell parameters for the HAPr sample ( $a = b = 9.408 \text{ \AA}$ ,  $c = 6.875 \text{ \AA}$ ) are slightly lower than those found

in theory ( $a = b = 9.419 \text{ \AA}$ ,  $c = 6.88 \text{ \AA}$ ). The volume of the cell ( $526.96 \text{ \AA}^3$ ) is also slightly below the theoretical value ( $529.16 \text{ \AA}^3$ ). Atom positions and distances between atoms in this sample are consistent with those of theoretical sample (Tables 4 and 5), which enables to have confidence in the refinement procedure. However, angles values of the tetrahedral  $\text{PO}_4$  show perturbation compared with the theoretical value; we can notice a slight decrease of O1-P-O2 angle and a slight increase of O3-P-O3 angle compared to theoretical value. Occupancy rate for O1 and O3 (Table 5) are slightly higher than the theoretical values (Table 7). We can also notice that the values of the factor (B) for O, H and P atoms, are lower or equal to 1 whereas they exceed 1 for calcium Ca1 (1.364) and Ca2 (1.524) (Table 5). The  $R_c$  value  $1.173 \text{ \AA}$  is near to the theoretical one ( $R_c = 1.177 \text{ \AA}$ ) while the distortion index ( $D_{ind} = 0.488$ ) is dramatically lower than found for the theoretical value ( $D_{ind} = 3, 079$ ) (Table 3).

**Table 3:** Distortion index  $D_{ind}$ , Volume and  $R_c$  values of HAPr, trace ions substituted and theoretical Hydroxyapatite

Sample	HAP	HAPr	HAP <sub>THE</sub>
$D_{ind}$	3.204	0.488	3.079
$R_c (\text{\AA})$	1.178	1.173	1.177
$V (\text{\AA}^3)$	526.74	526.96	529.16

For HAP synthetic apatite with trace ions, the cell parameters ( $a = b = 9.408 \text{ \AA}$ ,  $c = 6.872 \text{ \AA}$ ) are slightly lower than those found in theory ( $a = b = 9.419 \text{ \AA}$ ,  $c = 6.88 \text{ \AA}$ ). Distances between calcium and oxygen atoms present a disturbance: we can notice Ca2-O2 distances increase; Ca1-O1 and Ca2-O3 distances decrease (Table 4). Phosphorus and calcium occupancy rate, given in Table 6, is slightly less than the theoretical value while the oxygen (O1, O2 and O3) occupancy rate is slightly greater than the theoretical value (Table 7). The B factor values are found well above 1 for the calcium Ca1, oxygen O1 and O3. The volume of the cell ( $526.76 \text{ \AA}^3$ ) is also slightly below the theoretical value ( $529.16 \text{ \AA}^3$ ) and Dint distortion indice ( $D_{ind} = 3.204$ ) is slightly larger as that calculated for the theoretical value ( $D_{ind} = 3.079$ ) (Table 3).

**Table 4:** Angles and interatomic distances with their standard deviations for HAP and HAPr

Angles and Interatomic distances	HAP	HAPr	HAP <sub>THE</sub>
P-O(1)	1.583(9)	1.566(9)	1.540(7)
P-O(2)	1.499(7)	1.537(1)	1.545(8)
P-O(3)	1.549(5)	1.507(1)	1.515(5)
O(1)-P-O(2)	110.9(9)	109.4(5)	111.4(6)
O(1)-P-O(3)*2	111.3(7)	110.1(3)	111.1(7)
O(2)-P-O(3)*2	108.0(5)	108.6(3)	109.3(7)
O(3)-P-O(3)	107.2(4)	109.8(2)	106.9(4)
Ca(1)-O(1)	2.377(5)	2.391(7)	2.401(8)
Ca(1)-O(2)	2.458(5)	2.457(1)	2.458(7)
Ca(1)-O(3)	2.806(7)	2.808(5)	2.809(5)
Ca(2)-O(3)	2.327(5)	2.341(0)	2.342(5)
Ca(2)-O(2)	2.379(7)	2.357(6)	2.349(8)
Ca(2)-OH	2.385(4)	2.373(6)	2.382(4)
Ca(2)-O(3)	2.493(6)	2.525(9)	2.514(5)
Ca(2)-O(1)	2.690(8)	2.682(0)	2.708(6)

**Table 5:** Atomic coordinates and equivalent isotropic displacement parameters of HAPr

Atom	x	sx	y	sy	z	sz	B	sB	Occ. socc.	Mult
Ca1	0.33330(0)		0.66670 ( 0)		0.00237( 80)		1.364(228)		0.328(0)	4
Ca2	0.24539(46)		0.99235(57)		0.25000( 0)		1.524(203)		0.503(0)	6
P	0.39923(63)		0.36599( 63)		0.25000( 0)		0.908(220)		0.499(0)	6
O1	0.32913(127)		0.48604(104)		0.25000( 0)		0.831(334)		0.515(0)	6
O2	0.58778(127)		0.46574(124)		0.25000( 0)		0.573(363)		0.488(0)	6
O3	0.34313(75)		0.25971( 76)		0.07062( 82)		1.000( 0)		1.049(0)	12
O4	0.00000( 0)		0.00000( 0)		0.19725(294)		1.000( 0)		0.167(0)	4
H	0.00000( 0)		0.00000( 0)		0.06080( 0)		1.000( 0)		0.167(0)	4

**Table 6:** Atomic coordinates and equivalent isotropic displacement parameters of prepared HAP

Atom	Chem	x/a	y/b	z/c	Biso	Occ	Mult
Ca1	Ca	0.3333	0.6667	0.0016	1.1257	0.3235	4
Ca2	Ca	0.2467	0.9928	0.2500	0.9550	0.4936	6
P	P	0.3985	0.3674	0.2500	0.9204	0.4925	6
O1	O	0.3261	0.4873	0.2500	1.3958	0.5076	6
O2	O	0.5825	0.4621	0.2500	0.9660	0.5195	6
O3	O	0.3414	0.2545	0.0686	1.1253	1.0036	12
O4	O	0.0000	0.0000	0.1956	0.3020	0.1666	4
H	H	0.0000	0.0000	0.0608	1.0000	0.1666	4

**Table 7:** Atomic coordinates and equivalent isotropic displacement parameters of the theoretical Hydroxyapatite

Atom	Chem	x/a	y/b	z/c	Biso	Occ	Mult
Ca1	Ca	0.33330	0.66670	0.00131	1.00000	0.33333	4
Ca2	Ca	0.24651	0.99311	0.25000	1.00000	0.50000	6
P	P	0.39831	0.36831	0.25000	1.00000	0.50000	6
O1	O	0.32822	0.48461	0.25000	1.00000	0.50000	6
O2	O	0.58761	0.46521	0.25000	1.00000	0.50000	6
O3	O	0.34331	0.25791	0.06933	1.00000	1.00000	12
O4	O	0.00000	0.00000	0.19787	1.00000	0.16665	4
H	H	0.00000	0.00000	0.06080	1.00000	0.16665	4

## 5. Discussion

The IR absorption, X-ray diffraction pattern and the chemical test result of reference sample (HAPr) and sample with ions trace (HAP) are similar. Both samples can be considered as pure hydroxyapatite.

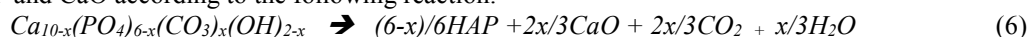
Results from chemical analysis for HAPr sample show Ca/P molar ratio close to the theoretical values and very low concentration of  $Mg^{2+}$ ,  $Na^+$  and  $Sr^{2+}$  ( $\Sigma$  ions traces 169 ppm) and 0.33 W % for carbonate mass fraction. Inclusion of  $CO_3^{2-}$  grouping in the lattice can explain the decrease of crystallographic parameters. The effect of carbonate ions on the structure of the hydroxyapatite has been extensively studied in the literature [18, 19]. It is well known that carbonate has been detected as an abundant trace element next to the presence of calcium and phosphorous in natural and in prepared apatite. Carbonates can be a substitute for the hydroxide ions (A-type substitution) and / or ion phosphates ( $\beta$ -type substitution). The generated materials will have a different profile of degradation and thermal stability [20, 21].

The B factor values greater than 1 for Ca1 and Ca2 atoms highlight the existence of vacancies at both Calcium sites (Table 5). This is due to the partial replacement of  $PO_4^{3-}$  grouping by  $CO_3^{2-}$  grouping. Indeed, the charge unbalance occurring when ( $CO_3^{2-}$ ) ions replace ( $PO_4^{3-}$ ) groups is primarily compensated by vacancies in Ca sites. The mechanism can be written as follows:



$V_{Ca}$  represents a vacancy on a hydroxyapatite lattice site occupied by Ca. The obtained product is hydroxyapatite with  $\beta$ -type substitution ( $Ca_{10-x}(PO_4)_6-x(CO_3)_x(OH)_2-x$ ).

According to the literature [20-22],  $\beta$ -type carbonated apatite dissociates at high temperature (800 to 1050°C) into a mixture of HAP and CaO according to the following reaction:



Chemical analysis performed on the samples calcined at 1100°C show the presence of carbonates and the chemical test confirms the absence of CaO. This result indicates that the prepared powders correspond to stable carbonated apatite to 1100 °C.

The phosphate group is more perturbed by carbonate substitution. In fact, the occupation rate of the oxygen atoms are affected (Table 5). We can also note a slight increase in the P-O1 distance and a slight decrease in P-O2 and P-O3 distance accompanied by O-P-O angle perturbation. The phosphorus atomic radius ( $r = 1.10 \text{ \AA}$ ) is higher than that of carbon ( $r = 0.76 \text{ \AA}$ ) and the volume of  $PO_4$  tetrahedron is higher than  $CO_3$  one. This leads to the reduction of the volume of the lattice and arrangement in the structure indicated by the index value calculated from the  $PO_4$  tetrahedral distortion ( $D_{ind} = 0.488$ ) well below the theoretical value ( $D_{ind} = 3.079$ ). The compound obtained present a vacancy structure in both sites of calcium (Ca1 and Ca2) induced by the partial substitution of phosphate ions by carbonate ions. The Rc value (Table 3) and the Ca2-OH distance (Table 4) indicate that the tunnel structure is slightly affected.

Chemical analysis, for calcined HAP sample with trace ions, is presented in Table 1. It reveals the presence of trace ions as  $Na^+$ ,  $Mg^{2+}$ ,  $Sr^{2+}$  and  $S^{2-}$  with total sum estimated to 612 ppm.

Calculated Ca/P molar ratio is close to the theoretical values whereas the calcium and phosphorus mass

fractions are slightly lower than the values found for reference sample (HAPr) and for the stoichiometric hydroxyapatite. These results reveal the substitution of calcium and phosphorus by trace ions and these substitutions did not seem to affect the diffraction pattern of prepared powders.

According to the reported work [23], an apatitic lattice contains always 6 groups  $\text{PO}_4^{3-}$  with the possible substitutions such as  $\text{SiO}_4^{4-}$ ,  $\text{CO}_3^{2-}$  and  $\text{SO}_4^{2-}$ ... Based on our chemical analysis, the  $\text{CO}_3^{2-}$  and  $\text{SO}_4^{2-}$  presence are confirmed (Table 1). We can note that the presence of traces cation ion favors the incorporation of carbonate ions. The O-P-O angles are slightly affected and the same changes are observed in the HAPr case with the inclusion of carbonate ions. In addition, the perturbation in the P-O distance is more marked in the hydroxyapatite case with trace ions. This marked variation can be explained by the simultaneous insertion of carbonate and sulphate ions in the lattice. Electric neutrality is ensured by reduction in the cation charge resulting from substitution of Ca2 site by trace cations, and vacancy creation in the Ca1 site. Structural changes lead to a disruption of the calcium-oxygen bonds lengths, since we can observe an increase of Ca2-O2 distances and decrease of the Ca1-O1 and Ca2-O3 distance. The B factor value of Ca1, O1 and O3 atoms also exceed 1 is due to the vacancies sites. Substitution of  $\text{PO}_4^{3-}$  by  $\text{CO}_3^{2-}$  and  $\text{SO}_4^{2-}$  in hydroxyapatite is accompanied with substitution at Ca2 position and vacancies at Ca1, O1 and O3 positions.

The effects of incorporation of the individual ion (as  $\text{Mg}^{2+}$ ,  $\text{Na}^+$ ,  $\text{Sr}^{2+}$ ,  $\text{CO}_3^{2-}$ ...) on the solubility, stability and crystalline structure have been studied in the literature [24-26]. Simultaneous insertion of cation and anion (as  $\text{Mg}^{2+}$ ,  $\text{Na}^+$ ,  $\text{Sr}^{2+}$ ,  $\text{Zn}^{2+}$  and  $\text{SiO}_4^{4-}$ ,  $\text{CO}_3^{2-}$ ) in hydroxyapatite lattice are also revealed and discussed [22, 27], but the effect of the insertion of some ion traces has not studied, and the limit of trace ions is not known. Generally the decomposition of prepared hydroxyapatite is promoted by the non-stoichiometry of the hydroxyapatite or the presence of impurities (as  $\text{Mg}^{2+}$ ,  $\text{CO}_3^{2-}$ ...). However we can note in this study, TGA and DTG curves of the sample presented in Figure 2, show the thermal stability of the structure pointing out that the sample decomposition takes place at 1450 °C. Coupled substitution of cations and anions traces, affect neither theoretical structure nor thermal stability of the hydroxyapatite but causes slight shift of OH position atom, decrease of crystallographic parameters and vacancies creation in calcium (Ca1) and oxygen (O1 and O3) sites. This structural change leads to a slight lattice distortion ( $D_{\text{ind}} = 3.204$ ) compared to the theoretical value ( $D_{\text{ind}} = 3.079$ ).

Synthetic hydroxyapatite is widely used in biomedical applications because of its excellent biocompatibility with tooth and bone tissues. The ions traces studied in this work are often detected in the synthetic hydroxyapatite and these elements are also present in biological apatite [28, 29]. These ions affect the dissolution of calcium-apatite and the formation and resorption of bone in vivo and in vitro [30-33].

The present work reveals the effect of these ions trace on the structural atomic rearrangement in prepared hydroxyapatite. The materials analyzed in this study, prepared under industrial conditions with low economic cost, appear very promising for biological applications.

## 6. Conclusion

This study reveals the effect of trace ions as  $\text{Mg}^{2+}$ ,  $\text{Na}^+$ ,  $\text{Sr}^{2+}$ ,  $\text{SO}_4^{2-}$ , and  $\text{CO}_3^{2-}$  on the stoichiometric hydroxyapatite structure. The powders were synthesized, under air atmosphere, by reaction between the calcium hydroxide and orthophosphoric acid at room temperature and neutral pH. The investigated by X-ray pattern fitting methods showed that in the absence of cation traces, the partial replacement of  $\text{PO}_4^{3-}$  by  $\text{CO}_3^{2-}$  groups leads to the relaxation of the lattice by creation of vacant calcium site. The  $\text{PO}_4^{3-}$  distortion index, ( $D_{\text{ind}} = 0.488$ ) is lower as that calculated for the theoretical value ( $D_{\text{ind}} = 3.079$ ). For trace ions substituted hydroxyapatite, the presence of traces cation ion favours the incorporation of carbonate ions and coupled substitution on calcium and phosphorus position affect neither theoretical structure nor thermal stability of the hydroxyapatite but causes structural atomic rearrangement leads to a slight lattice distortion ( $D_{\text{ind}}=3.204$ ). Composition and microstructure of analyzed materials prepared under industrial conditions appear very promising for biological applications.

## 7. References

- [1] A. Herts, I.J. Bruce, Nanomedicine, 2, 6 (2007) 899.
- [2] J. Barbarand, M. Pagel, Am. Mineral, 86 (2002) 473.
- [3] Z. L. Dong, T.J. White, B. Wei, K. Laursen, AM. Ceramic. Soc, 85 (2002) 2515.
- [4] R. Z. LeGeros, P.W. Brown, B. Constanz., Boca Raton, FL, 328, (1994).
- [5] O. Gauthier, J.M. Bouler, E. Aguado, R. Z. LeGeros, P. Pilet, G. Daculsi., J. mater. Med, 10 (1999) 199-204.
- [6] S. V. Dorozhkin, Review, Materials, 2 (2009) 399-498.
- [7] LeGeros, R.Z. Lin, S.; Rohanizadeh, R.; Mijares, D.; LeGeros, J.P. Biphasic calcium phosphate bioceramics: preparation, properties and applications. J. Mater. Sci. Mater. Med. (2003) 14, 201-209
- [8] Daculsi, G.; Laboux, O.; Malard, O.; Weiss, P. Current state of the art of biphasic calcium phosphate bioceramics. J. Mater. Sci. Mater. Med. (2003) 14, 195-200.
- [9] E. C. Moreno, K. Varughese, J. Cryst. Growth, 53, 20, (1981).
- [10] M. Akao, H. Aoki, K. Kato, J. Mater. Sci, 11, 809, (1981).

- [11] T. Kawasali, *J. Chromatogr.*, 544 (1991) 147-184.
- [12] S. Kannan, A. F. Lemos, J. M. F. Ferreira, *Mater.* 18 (2006) 2181-2186
- [13] T.I. Ivanova, O.V. Frank-Kamenetskaya, A.B. Kol'tsov, V.L. Ugolkov, *Journal of Solid*, 160 (2) (2001) 340-349
- [14] F. Abida, dissertation , Ph.D, UCD, Maroc ( 2011).
- [15] L. Bernard, M. Freche, J.L. Lacout, B. Biscans, *Chemical Engineering Science* 55 (2000) 5683-5692.
- [16] J. Rodriguez Carvajal, *Physica B* 192 (1993) 55.
- [17] K. Sudarsanan, R.A. Young, *Acta Crystallographica B.* 25 (1969) 1534- 1543.
- [18] H. El Feki, J.M. Savariault, A. Ben Salah, *Alloys Compd.* 287 (1999) 114–120.
- [19] M. Veiderma, K. Tonsuaadu, R. Knubovets, M. Peld. *Journal of Organometallic Chemistry*, 690 (2005) 2638–2643.
- [20] J.P. Lafon, E. Champion, D. Bernache Assolant, *Matériaux* (2002).
- [21] J. C. Labarth, G. Bonel; G. Montel, *Ann. Chim.* 8 (1973) 289-301.
- [22] H. El Feki, J. M. Savariault, A. Ben Salah, M. Jemal, sodium and carbonate distribution in substituted calcium Hydroxyapatite, *Solid State Sciences* 2 (2000) 577–586
- [23] G. Montel, 230 (1973),13-18
- [24] J.C. Elliot, in: *Calcium Phosphate Materials. Fundamentals*, Sauramps Medical (1998), pp. 25–26.
- [25] R.Z. Legeros, in: R.W. Fearnhead, S. Suga (Eds.), *Tooth Enamel IV*, Elsevier, Amsterdam, (1984), pp. 32–36.
- [26] T. Turki, A. Aissa, H. Agougui, M. Debbabi , *Journal de la Société Chimique de Tunisie* (2010) 12, 161-172.
- [27] M. Veiderma, K. Nsuaadu, R. Knubovets, M. Peld, *Journal of Organometallic Chemistry* 690 (2005) 2638–2643.
- [28] J.C Elliot, in “structure in Inorganic Chemistry 18 : Structure and chemistry of the Apatite and Other Calcium Orthophosphates” Elsevier, Amsterdam, (1994) p. 111.
- [29] D. K. Smith, in “Hydroxyapatite and Related Materials” edited by P.W. Brown and B. Constanz (CRC Press, London ) (1994)
- [30] M. Jamil, F. Abida, Z. Hatim, M. Ellassfour and E. Gourri, Effects of ions traces on the dissolution of bioceramics composed of hydroxyapatite and  $\beta$ -tricalcium phosphate. *Mediterranean Journal of Chemistry* (2015) 4(1), 51-58
- [31] M. Jamil, B. El ouatli, A. Elouahli, F. Abida, Z. Hatim, *International Journal of Scientific & Engineering Research*, Volume 7, Issue 1, January (2016).
- [32] F.S.Kaplan, W.L. Hayes, T. M. Keaveny, A. Boskey, T.A. Einhor and J.P. Iannotti, in” *Orthopedic Basic Research*”, Edite by S.P. Simon (American Academy of Orthopedic Surgeons ) (1994) p. 127.
- [33] A. Allison, M. L. Campbell, G. H. Nancollas, The influence of carbonate and magnesium ions on the growth of hydroxyapatite, carbonated apatite and human powdered enamel *Colloids and Surfaces*, 54 (1991) 25.-31